OXFORD

SOT | Society of Toxicology
www.toxsci.oxfordjournals.org

TOXICOLOGICAL SCIENCES, 142(2), 2014, 403–417

doi: 10.1093/toxsci/kfu187
Advance Access Publication Date: September 19, 2014

Inhaled Diesel Emissions Generated with Cerium Oxide Nanoparticle Fuel Additive Induce Adverse Pulmonary and Systemic Effects

Samantha J. Snow*,†,1, John McGee†, Desinia B. Miller*, Virginia Bass‡, Mette C. Schladweiler†, Ronald F. Thomas†, Todd Krantz†, Charly King†, Allen D. Ledbetter†, Judy Richards†, Jason P. Weinstein§, Teri Conner§, Robert Willis§, William P. Linak¶, David Nash¶,||, Charles E. Wood|||, Susan A. Elmore||||, James P. Morrison#, Crystal L. Johnson#, Matthew Ian Gilmour†, and Urmila P. Kodavanti†

*Curriculum in Toxicology, University of North Carolina at Chapel Hill, Chapel Hill, North Carolina, 27599, †Environmental Public Health Division, NHEERL, US Environmental Protection Agency, Research Triangle Park, North Carolina, 27711, ‡Department of Environmental Science and Engineering, Gillings School of Public Health, University of North Carolina at Chapel Hill, Chapel Hill, North Carolina, 27599, §Environmental Characterization and Apportionment Branch, NERL, US Environmental Protection Agency, Research Triangle Park, North Carolina, 27711, ¶Air Pollution Prevention and Control Division, NRMRL, US Environmental Protection Agency, Research Triangle Park, North Carolina, 27711, ||Arcadis US Inc., Durham, North Carolina, 27713, |||Integrated Systems Toxicology Division, NHEERL, US Environmental Protection Agency, Research Triangle Park, North Carolina, 27711, ||||National Toxicology Program Division, National Institute of Environmental Health Sciences, Research Triangle Park, North Carolina, 27711 and #Pathology Associates Inc., Charles River Laboratories, Durham, North Carolina, 27703

[1]To whom correspondence should be addressed at Environmental Public Health Division, NHEERL, US Environmental Protection Agency, 109 T.W. Alexander Dr., Research Triangle Park, NC 27711. Fax: 919 541 0026. E-mail: snow.samantha@epa.gov.

Disclaimer: The research described in this article has been reviewed by the National Health and Environmental Effects Research Laboratory, U.S. Environmental Protection Agency and approved for publication. Approval does not signify that the contents necessarily reflect the views and the policies of the agency, nor does mention of trade names of commercial products constitute endorsement or recommendation for use.

ABSTRACT

Diesel exhaust (DE) exposure induces adverse cardiopulmonary effects. Cerium oxide nanoparticles added to diesel fuel (DECe) increases fuel burning efficiency but leads to altered emission characteristics and potentially altered health effects. Here, we evaluated whether DECe results in greater adverse pulmonary effects compared with DE. Male Sprague Dawley rats were exposed to filtered air, DE, or DECe for 5 h/day for 2 days. N-acetyl glucosaminidase activity was increased in bronchial alveolar lavage fluid (BALF) of rats exposed to DECe but not DE. There were also marginal but insignificant increases in several other lung injury biomarkers in both exposure groups (DECe > DE for all). To further characterize DECe toxicity, rats in a second study were exposed to filtered air or DECe for 5 h/day for 2 days or 4 weeks. Tissue analysis indicated a concentration- and time-dependent accumulation of lung and liver cerium followed by a delayed clearance. The gas-phase and high concentration of DECe increased lung inflammation at the 2-day time point, indicating that

gas-phase components, in addition to particles, contribute to pulmonary toxicity. This effect was reduced at 4 weeks except for a sustained increase in BALF γ-glutamyl transferase activity. Histopathology and transmission electron microscopy revealed increased alveolar septa thickness due to edema and increased numbers of pigmented macrophages after DECe exposure. Collectively, these findings indicate that DECe induces more adverse pulmonary effects on a mass basis than DE. In addition, lung accumulation of cerium, systemic translocation to the liver, and delayed clearance are added concerns to existing health effects of DECe.

Key words: diesel exhaust; cerium oxide; cardiopulmonary; nanoparticle

Epidemiological and experimental studies have indicated a strong association between air pollution exposure and adverse cardiopulmonary morbidity and mortality (Brunekreef and Holgate, 2002; Stanek *et al.*, 2011). Diesel exhaust (DE) contributes to overall air pollution and has been extensively studied for adverse health outcomes in humans and animals (Ghio *et al.*, 2012; Hesterberg *et al.*, 2009b; Ristovski *et al.*, 2012). Acute exposures to DE have been shown to increase pulmonary inflammation, alter systemic vascular reactivity and contractility, and promote myocardial ischemia (Cosselman *et al.*, 2012; Mills *et al.*, 2007; Salvi *et al.*, 1999; Wauters *et al.*, 2013). Increasing demand of travel, widespread availability of diesel fuels, and stricter emission standards have necessitated the development of alternative fuel technologies. Among these technologies are methods to increase fuel burning efficiency and decrease particulate matter (PM) emission, including the use of fuel borne catalysts, particulate filters, and renewable energy sources, such as ethanol and biofuels (HEI, 2001; Neeft *et al.*, 1996).

Cerium oxide (CeO_2) nanoparticles are increasingly being used as a fuel borne catalyst in Europe, North America, and elsewhere (Cassee *et al.*, 2011; Johnson and Park, 2012; Wakefield *et al.*, 2008). Ce-based fuel borne catalysts increase fuel burning efficiency, decrease exhaust emission of PM on a mass basis, reduce the number of particles in the accumulation mode (diameter of 0.1–2.5 μm), increase the number of ultrafine particles emitted (diameter <0.1 μm), and alter the emission levels of several gaseous pollutants (HEI, 2001; Jung *et al.*, 2005; Skillas *et al.*, 2000; Zhang *et al.*, 2013). Metal fuel borne catalysts, which may also include iron and platinum for diesel applications, are often intended for use in combination with specialized diesel particulate filters (DPFs) that effectively trap the metals. However, they may also be used without DPFs where the metals can contribute to environmental emissions and elevate metal concentrations in the air, soil, and water (HEI, 2001; Johnson and Park, 2012; O'Brien and Cummins, 2010). These metal fuel borne catalysts form nanoparticles during combustion and are effective in promoting soot oxidation and reducing mass emissions though they can also lead to increases in particle number emissions. Further details describing metal fuel borne catalyst behavior and mechanisms in diesel systems are discussed by Nash *et al.* (2013).

Exposure to nanoparticles leads to different toxicological profiles than larger sized particles because of their large surface area-to-mass ratio, increased reactivity, and altered deposition, absorption, translocation, and elimination rates (Geraets *et al.*, 2012; Shannahan *et al.*, 2012). Studies using *in vitro* cellular models or *ex vivo* lung slices have resulted in conflicting findings following exposure to CeO_2 nanoparticles. Several investigators have reported that CeO_2 nanoparticles are protective against agonist- or ROS-induced cell cytotoxicity, apoptosis, and oxidative stress (Chen *et al.*, 2013; Hirst *et al.*, 2009), whereas others have shown minimal to no change in cell viability, cell morphology, or markers of inflammation and oxidative damage (Fall *et al.*, 2007; Park *et al.*, 2007, 2008a). Additional studies have demonstrated that exposure to CeO_2 nanoparticles increase cell cytotoxicity, oxidative stress, inflammation, apoptosis, and autophagy (Eom and Choi, 2009; Gojova *et al.*, 2009; Hussain *et al.*, 2012; Lin *et al.*, 2006; Park *et al.*, 2008b). *In vivo*, exposure to CeO_2 nanoparticles leads to translocation and accumulation of Ce in extrapulmonary organs including the liver, kidney, and spleen (Geraets *et al.*, 2012; He *et al.*, 2010; Hirst *et al.*, 2013; Yokel *et al.*, 2009), as well as induction of pulmonary and hepatic toxicity (Ma *et al.*, 2011; Nalabotu *et al.*, 2011; Srinivas *et al.*, 2011). Collectively, these studies suggest Ce inhaled along with DE, as a result of CeO_2 nanoparticle fuel additive (DECe) use, may result in distinct health consequences compared with exposure to DE alone.

There are only a small number of comparative animal studies investigating the differences in cardiopulmonary and systemic health effects following exposure to DE and DECe. Cassee *et al.* (2012) demonstrated that exposure to DE increased the atherosclerotic burden in atherosclerosis-prone mice that was not seen following exposure to DECe, however, only DECe exposure resulted in elevated neuroinflammation in the cerebellum and brain stem. In a study conducted by Ma *et al.* (2014), it was shown that CeO_2 nanoparticles and DECe led to increased and sustained lung injury in rats compared with DE alone. Clearly, the potential adverse health effects from exposure to DE with the addition of CeO_2 nanoparticles are not yet fully understood. The objectives of our study were to (1) compare the pulmonary toxicity following exposure to DE and DECe and (2) characterize the tissue deposition of Ce and cardiopulmonary toxicity following DECe exposure for 2 days or 4 weeks with and without a 14-day recovery period. We hypothesized that the addition of CeO_2 nanoparticles to diesel fuel would result in lung accumulation and systemic translocation of Ce, and cause greater adverse pulmonary health effects compared with DE exposure alone.

MATERIALS AND METHODS

Animals. Healthy male Sprague Dawley rats (8 weeks old) were purchased from Charles River Laboratories Inc (Raleigh, North Carolina). Animals were housed (2 per cage) in polycarbonate cages containing beta chip bedding and acclimatized for 2–3 weeks in an Association for Assessment and Accreditation of Laboratory Animal Care-approved animal facility ($21 \pm 1^{\circ}$C, $50 \pm 5\%$ relative humidity [RH], and 12 h light/dark cycle). Rats were then transported to a nearby satellite animal facility where they were single housed in polycarbonate individually ventilated cages with beta chip bedding. Animals received standard (5001) Purina rat chow (Brentwood, Missouri) and water ad libitum except during exposures. The U.S. EPA NHEERL Institutional Animal Care and Use Committee approved all procedures in this protocol.

Generation and characterization of DE and DECe exhaust. DE for exposure experiments was generated using a 4.8-kW (6.4 hp) direct injection single-cylinder 0.320 l displacement Yanmar L70 V diesel generator operated at a constant 3600 rpm. Resistance heating elements provided a constant 3 kW load. While the engine is not representative of newer technologies, it does represent an important set of legacy technologies likely to remain in use for decades. This system was chosen because it is inexpensive, quickly replaceable in case of malfunction during long-term exposure studies, and because small diesel systems have been used by other groups to study fuel borne catalysts (Miller *et al.*, 2007) and comparative health effects (Campen *et al.*, 2005; McDonald *et al.*, 2011). The base fuel was ultralow sulfur diesel (ULSD, <15 ppm sulfur), purchased locally (Red Star Oil, Raleigh, North Carolina), while the Ce modified fuel was prepared by adding the product Envirox (Energenics Europe Ltd, Kidlington, Oxfordshire, United Kingdom) to achieve a 10-ppm Ce by weight concentration. In the United States, ULSD was phased in for on-road use from 2006 to 2010, and has been used exclusively since December 1, 2010.

For the first exposure experiment, two identical engines and dilution systems were used. One engine was fueled with base ULSD, and the other was fueled with the same ULSD with Ce additive. These dilution systems consisted of single eductors (Air-Vac, Model TD26OH, Seymour, Connecticut) operating near the engine exhaust port, which directed diluted DE without and with Ce additive (DE and DECe) to two Hazelton 1000 (984 l) exposure chambers housed in an isolated animal exposure room. Both eductors were fitted with an orifice that drew in approximately 2 l/min of DE while using 28 l/min of high efficiency particulate air (HEPA) filtered dilution air. The resulting dilution ratio (14:1 dilution) resulted in target particle exposure concentrations of approximately 1000 $\mu g/m^3$. A third control chamber was supplied with HEPA filtered room air.

For the second exposure experiment, two different dilution systems were used simultaneously on a single engine to provide whole emissions to two exposure chambers. These two dilution systems created low (approximately 100 $\mu g/m^3$) and high (approximately 1000 $\mu g/m^3$) concentration DECe. High concentration exhaust was also directed through a HEPA filter to a third chamber to examine particle free gas-phase diesel emissions. To generate sufficient sample volumes for both the high concentration DECe and HEPA filtered gas-phase exposures, a different dilution system was used. This system diluted approximately 85 l/min of engine exhaust with approximately 1200 l/min (14:1 dilution) of HEPA filtered air through a cone diluter as previously described (Gowdy *et al.*, 2010; Sharkhuu *et al.*, 2010). The low concentration DECe exposure used the same eductor dilution system described earlier for the first exposure experiment. However, dilution flows were increased (140:1) to achieve particle concentrations and residence times sufficiently low to preserve an ultrafine mode created by the Ce catalyst. A fourth control chamber received HEPA filtered room air.

All chamber concentrations (exhaust dilutions) were controlled by periodic adjustments of dilution air based on continuous mass concentrations determined by a tapered element oscillating microbalance (TEOM; Rupprecht and Patashnick Co., series 1400, Albany, New York). Particle size distributions (PSDs) were characterized during each exposure using a scanning mobility particle sizer spectrometer (SMPS; TSI Inc, Model 3080/3022a, St. Paul, Minnesota). Continuous emission monitors were used to measure chamber concentrations of PM and gas components as described elsewhere (Gordon *et al.*, 2012). Chamber temperatures, RH, and noise were also monitored. The organic carbon/elemental carbon ratio of 0.6 for the particulate fraction of DE using similar fuel and combustion conditions have been reported (Sharkhuu *et al.*, 2010).

Animal exposures. Two exposure experiments were conducted. In the first experiment, rats were exposed to filtered air, DE, or DECe (high concentration; approximately 1000 $\mu g/m^3$) for 5 h/day × 2 consecutive days. In the second experiment, rats were exposed to filtered air, DECe at a low concentration (approximately 100 $\mu g/m^3$), DECe at a high concentration (approximately 1000 $\mu g/m^3$), or the gas-phase components of the high concentration of DECe for 5 h/day × 2 consecutive days or 5 h/day × 5 days/week × 4 weeks. The 2-day exposure time point was chosen to assess acute effects, while the 4-week time point was selected to evaluate the persistency and progressive nature of these potential effects. A group of rats exposed to filtered air or DECe (high concentration) were allowed a 14-day recovery period after the 4-week exposure to determine reversibility of health effects. All necropsies for both experiments were performed 1 day after the final exposure.

Necropsy and sample collection. At designated time points, rats were weighed and anesthetized with an overdose of sodium pentobarbital (50–100 mg/kg, ip; Virbac AH, Inc, Fort Worth, Texas). Blood was collected via abdominal aortic puncture directly into vacutainers (Sigma-Aldrich, St. Louis, Missouri) containing citrate for platelet aggregation assay or EDTA for complete blood counts (CBC). The trachea was cannulated, and the left lung and right cardiac lobe were ligated while lavaging the remaining three right lung lobes (apical, diaphragmatic, and azygous). The three right lung lobes were lavaged with Ca^{2+}/Mg^{2+} free phosphate buffered saline (pH 7.4, 37°C) using a 10-ml syringe. The lavage volume was based on 28 ml/kg body weight, with the three right lung lobes representing 50% of the total lung weight. Three washes were performed with the same buffer aliquot. The bronchoalveolar lavage fluid (BALF) was stored in 15 ml sterile tubes on ice until processing. The left lung was inflated with 10% formalin and processed for histopathology. The right cardiac lobe and a consistent portion of a given liver lobe from each animal were frozen in liquid nitrogen and stored at −20°C for later analysis of tissue Ce burden. The thoracic aorta was isolated from surrounding connective tissues and quick frozen in liquid nitrogen for later RNA isolation and PCR.

Cell differential and BALF analysis. For both experiments, aliquots of BALF were used to determine total cell counts with a Z1 Beckman-Coulter Counter (Beckman-Coulter, Inc, Miami, Florida) and cell differentials according to previously described procedures (Gordon *et al.*, 2013). The cell-free BALF was used to analyze lung injury biomarkers total protein, albumin, lactate dehydrogenase (LDH) activity, N-acetyl glucosaminidase (NAG) activity, and γ-glutamyl transferase (GGT) activity as previously described (Gordon *et al.*, 2013).

Filter and tissue Ce analysis. Gelman Teflo filters (1 μm nominal pore size, 47 mm diameter; Pall Gelman Sciences, Ann Arbor, Michigan) containing deposited DECe during daily exposures, along with lot-matched blank filters, were analyzed for Ce content using energy dispersive X-ray fluorescence spectrometry (EDXRF; Model Epsilon 5, PANalytical, Westborough, Massachusetts). The analytical method followed the principles of the U.S. EPA Method IO-3.3 (EPA, 1997).

Lung (approximately 0.1 g) and liver (approximately 0.5 g) samples were weighed and microwave digested (Yokel *et al.*, 2009)

with a mixture of concentrated HNO_3 (1.5 ml) and H_2O_2 (0.75 ml) (Optima grades; Fisher Scientific, Pittsburgh, Pennsylvania) in 10 ml Teflon vessels (SP-D; CEM Corporation, Matthews, North Carolina). Sample digests were transferred to acid-cleaned 15 ml polypropylene centrifuge tubes, and diluted using a solution of 0.4% H_2SO_4 (10 ml) (Optima grade; Fisher Scientific) in ultrapure water (Milli-Q; Millipore Corporation, Billerica, Massachusetts). Ce content was measured using inductively coupled plasma-mass spectrometry (ICP-MS; Model ELAN DRCII, PerkinElmer, Shelton, Connecticut). Ce is not an analyte in standardized environmental ICP-MS methods; however, we followed the quality control and run sequence of U.S. EPA Method 200.8, rev 5.4 (EPA, 1994) to achieve study data quality objectives. Ce isotopes 140 (reported) and 142 (confirmation) were monitored, and indium and terbium internal standards were spiked into all samples, blanks, and standards using an online mixer. Calibration (PCEN-100; VHG Labs, Manchester, New Hampshire) and quality control (PLCE2-2 Y; Spex CertiPrep, Metuchen, New Jersey) standards were diluted with an acid blank solution that was matrix-matched with the samples. Detection limits of 0.22 ng Ce/g lung tissue and 0.38 ng Ce/g liver tissue were achieved.

Pulmonary deposition estimation. The multiple-path particle dosimetry modeling software (MPPD v 2.11; Applied Research Associates, Inc, Albuquerque, New Mexico) was used to predict the pulmonary deposition fraction of particles for the animals exposed to the low concentration and high concentration of DECe for 2 days and 4 weeks. Default rat-specific values provided by the software including functional residual capacity volume (4.0 ml), upper respiratory tract volume (0.42 ml), head volume (0.42 ml), and inspiratory fraction (0.5), along with the average experimental-specific data for tidal volume (V_T, 2.5 ml) and breathing frequency (f, 208 breaths/min), obtained using a whole-body plethysmography (Buxco Electronics, Inc, Sharon, Connecticut) as previously described (Kodavanti *et al.*, 2006), were inputed into the model. Whole-body plethysmography was performed prior to the start of exposure, 2 days post-exposure, and after 19 days of exposure for the 4-week group. No major exposure-related effects on breathing parameters were noted. For the particle properties, density was estimated to be 1.0 g/cc (Yoon *et al.*, 2011) with a geometric standard deviation (σ_g) of 1.70 for the low chamber and 1.45 for the high chamber. The concentration and mass median aerodynamic diameter for each exposure group were determined by TEOM and SMPS, respectively, as described earlier.

The estimated pulmonary deposition of PM was calculated from the following equation as previously described (Wichers *et al.*, 2006):

$$D_{PM} = C \times f \times V_T \times t \times d_f \times U_{PM}$$

where D_{PM} = pulmonary deposition of PM in the total lung (μg), C = average concentration of PM (μg/m^3), f = breathing frequency (breaths/min), V_T = tidal volume (ml), t = total time of exposure (min), d_f = pulmonary deposition fraction for the total lung as predicted by the MPPD model, and U_{PM} = unit conversion (1×10^{-6} m^3/ml).

The estimated pulmonary deposition of Ce was calculated from the following equation:

$$D_{Ce} = D_{PM} \times P_{Ce} \times U_{Ce}$$

where D_{Ce} = pulmonary deposition of Ce in the total lung (ng), P_{Ce} = percent of Ce present in PM as calculated based on XRF analysis of the chamber filters, and U_{Ce} = unit conversion (1×10^3 ng/μg).

Lung histology and transmission electron microscopy. Left lungs were collected at necropsy for histopathology. After removal and inflation with 10% neutral buffered formalin (NBF), the lungs were placed whole in 10% NBF followed by 80% ethanol. Fixed lungs were paraffin-embedded, sectioned longitudinally at 5 μm, and stained with hematoxylin and eosin (H&E) using standard histological procedures. One H&E-stained section per animal was evaluated by a board-certified pathologist. Semi-quantitative scoring of select pathological findings was conducted using severity scores: 0 = not present, 1 = minimal (<10% of examined area), 2 = mild (11–40%), 3 = moderate (41–80%), and 4 = marked (81–100%). Images of representative lung sections were taken using a Nikon Eclipse E400 microscope (Nikon Instruments, Melville, New York) and Lumenera Infinity2 digital camera (Ottawa, Ontario).

Selected formalin fixed lung tissue samples from the second experiment were processed through an industry standard transmission electron microscopy (TEM) processing protocol per Charles River Laboratories, Pathology Associates Inc (Durham, North Carolina) and embedded in Spurr's epoxy resin. Approximately 1 μm thick sections were cut on one of two ultra microtomes (Reichert-Jung Ultracut E; Leica Microsystems, Vienna, Austria; RMC Powertome X; Boeckeler Instruments, Tucson, Arizona), placed on glass slides, and stained with toluidine blue for histological examination and for final tissue area selection for TEM. The selected areas were sectioned at approximately 80 nm thickness, placed on 200 mesh copper grids, and stained with uranyl acetate and lead citrate using standard protocols to enhance contrast on the electron microscope (Zeiss 900 Transmission Electron Microscope, Thornwood, New York). Photomicrographs were captured from selected fields at magnifications of ×4270–96 800 to characterize ultrastructural changes in the lung.

In vitro *platelet aggregation and CBC.* Citrated blood was centrifuged at 200 × g for 30 s. An aliquot of the platelet-rich plasma was collected, and the remaining sample was centrifuged at 2000 × g for 2 min to collect a platelet-poor fraction of plasma. Adenosine diphosphate (ADP)-induced primary aggregation and rates of aggregation and disaggregation were measured by adding 25 μl of ADP (1×10^{-4} M) to the platelet-rich plasma fraction at 37°C using a platelet aggregation profiler (Platelet Aggregation Profiler Model PAP-8E, Bio/Data Corp, Horsham, Pennsylvania). The light transmission set by the absorbance of the platelet-poor plasma fraction was used to blank each individual sample. Plasma samples from each individual animal were run in duplicate, and an average of the replicate values was used. CBC of EDTA containing blood tubes were performed using a Beckman-Coulter AcT blood analyzer (Beckman-Coulter Inc).

RNA isolation and real time reverse transcriptase PCR. Thoracic aortas from the second experiment (4-week time point) were used for determination of mRNA expression levels for markers of inflammation, vascular activity, and coagulation/thrombosis. Total thoracic aorta RNA was isolated with a commercially available RNeasy mini kit (Qiagen, Valencia, California) using silica gel membrane purification. RNA yield was determined spectrophotometrically on a NanoDrop 1000 (Thermo Scientific, Wilmington, Delaware). Reverse transcriptase PCR (RT-PCR) was conducted on an ABI Prism 7900 HT sequence detection system

(Applied Biosystems Inc, Foster City, California) as previously described (Gordon *et al.*, 2013). Primers were purchased from ABI as inventoried TaqMan Gene Expression Assays, each containing a 6-carboxy-fluorescein (FAM dye) label at the 5′ end. Data were analyzed using ABI sequence detection software version 2.2. For each PCR plate, cycle threshold (Ct) was set to an order of magnitude above background. For each individual sample, target gene Ct was normalized to a control gene Ct, hypoxanthine-guanine phosphoribosyltransferase (Hprt1), to account for variability in the starting RNA amount. Expression of each exposure group was quantified as fold change over filtered air control.

Statistical analysis. Statistical analysis was performed using GraphPad Prism (GraphPad Software, San Diego, California). One-way ANOVA analysis followed by Bonferroni's post hoc test was used to compare differences between exposure groups at each time point or concentration. The data from each experiment and at each time point were independently analyzed. A *t* test was used to compare differences between the animals exposed to filtered air or high concentration of DECe for 4 weeks and allowed a 14-day recovery period. A p-value $<.05$ was considered statistically significant.

RESULTS

Exposure Characterization

Figure 1A presents SMPS volume PSDs comparing emission measurements of the base ULSD (DE) and the ULSD with 10 ppm Ce (DECe). Standard deviations of multiple PSDs are included. These PSDs were determined from eductor diluted samples corrected back to engine stack concentrations as previously described (Nash *et al.*, 2013). Volume PSDs are calculated from the measured SMPS number distributions, assuming spherical particles with unit density, and provide an estimate of the relative change in mass emissions, and the distribution of mass across the PSD. Evident from Figure 1A is that the Ce fuel borne catalyst is effective in reducing engine volume/mass emissions. The SMPS data indicate that total volume concentrations decrease 40% (from 2.1×10^{13} to 1.2×10^{13} nm^3/cm^3) with the Ce additive. However, these same data also indicate particle number concentrations increase 27% (from 1.1×10^8 to 1.4×10^8 $\#/cm^3$) with the addition of the Ce nanoparticles. These particles are associated with an ultrafine particle mode seen in the 10 ppm Ce PSD between 15 and 35 nm. While these particles add little to the total volume or mass, and are minor compared to volume reductions in the larger accumulation mode, they dominate the number distribution. Median diameters for the 0 and 10 ppm Ce PSDs are 51 nm (number) and 104 nm (volume), and 29 nm (number) and 94 nm (volume), respectively.

The target DE and DECe particulate concentrations were either 1000 (high concentration) or 100 (low concentration) μg of PM/m^3. Actual PM mass concentrations, the chamber gas components, and atmospheric variables are provided in Table 1. In the first exposure experiment comparing high concentration exposures, average DE and DECe levels were 1000 and 800 $\mu g/m^3$, respectively (Table 1). The gas components CO, NO, and NO_2 from the DECe chamber were also decreased. In the second exposure experiment characterizing the cardiopulmonary effects of DECe, we examined the low concentration condition because it preserved a bimodal PSD into the exposure chamber, and we wanted to examine possible effects due to this characteristic. Figure 1B presents number PSDs comparing DECe particles from the low and high concentration exposure chambers. Note that the high concentration PSD does not indicate bimodal behavior or the presence of the ultrafine mode seen in the engine exhaust (Fig. 1A). This is due to the speed of aerosol kinetics and the distance and residence time (several seconds) required to transport aerosol emissions from the engine exhaust to the isolated exposure chambers. At 1000 $\mu g/m^3$, the kinetics are too fast to preserve the bimodal PSD observed in the exhaust (Fig. 1A). Additional dilution (to approximately 100 $\mu g/m^3$) slowed aerosol interaction, and preserved the bimodal PSD into the exposure chamber. The total number concentration and number median diameter for the high concentration exposure was 2.0×10^6 $\#/cm^3$ and 79 nm, respectively. Corresponding values for the low concentration exposure was 9.3×10^5 $\#/cm^3$ and 31 nm, respectively. However, the bimodal PSD indicates separate modes with medians of approximately

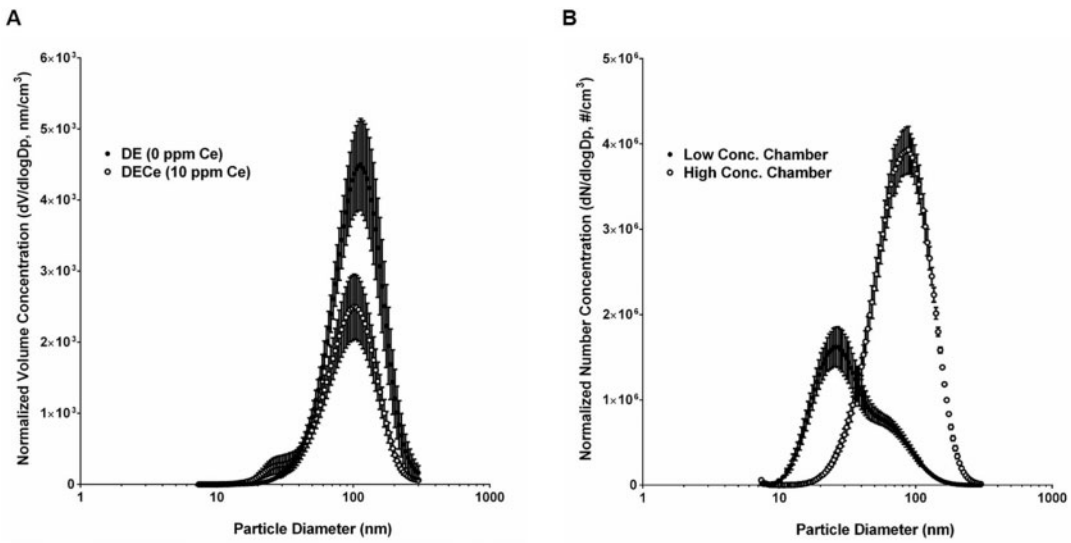

FIG. 1. Scanning mobility particle sizer spectrometer particle size distributions measured in the diesel engine exhaust and exposure chambers. A, Particle volume distributions calculated from measured particle number distributions and corrected for dilution to engine exhaust concentrations comparing emissions without (diesel exhaust [DE]: 0 ppm) and with (cerium oxide nanoparticles added to diesel fuel [DECe]: 10 ppm) Ce additive. B, Particle number distributions measured from the low concentration and high concentration exposure chambers. Average values with standard deviations are presented.

TABLE 1. Chamber Operating Conditions during 2-Day and 4-Week Exposure of Rats to Filtered Air, DE, and DECe

Chamber parameter	Filtered air	DE (high concentration)	DECe (high concentration)	
2-Day exposure comparing DE and DECe				
PM mass, TEOM ($\mu g/m^3$)	0.5 ± 1.4	1015.3 ± 103.2	798.1 ± 12.2	
O_2 (%)	20.8 ± 0.3	20.7 ± 0.2	20.8 ± 0.3	
CO (ppm)	1.7 ± 0.3	11.8 ± 1.4	9.3 ± 0.6	
NO (ppm)	0.3 ± 0.2	5.1 ± 0.5	3.5 ± 0.1	
NO_2 (ppm)	0.3 ± 0.1	0.5 ± 0.2	0.4 ± 0.1	
Temperature (°F)	68.9 ± 0.7	76.8 ± 0.2	71.3 ± 0.4	
RH (%)	54.8 ± 0.1	37.1 ± 0.3	32.2 ± 0.3	
Chamber parameter	**Filtered air**	**DECe (gas-phase)**	**DECe (low concentration)**	**DECe (high concentration.)**
2-Day DECe exposure				
PM mass, TEOM ($\mu g/m^3$)	1.4 ± 0.2	27.4 ± 8.4	66.4 ± 9.4	1003.5 ± 31.6
O_2 (%)	21.0 ± 0.1	20.1 ± 0.4	21.0 ± 0.1	20.0 ± 0.4
CO (ppm)	0.2 ± 0.1	40.5 ± 15.8	3.4 ± 0.6	39.3 ± 18.5
NO (ppm)	0.2 ± 0.1	37.0 ± 4.8	3.3 ± 0.9	36.5 ± 8.9
NO_2 (ppm)	0.4 ± 0.3	5.5 ± 1.2	1.0 ± 0.3	4.1 ± 1.4
Temperature (°F)	74.7 ± 0.6	73.0 ± 0.5	74.0 ± 0.4	72.4 ± 0.3
RH (%)	41.8 ± 5.3	49.3 ± 2.9	48.9 ± 3.6	36.4 ± 0.7
Chamber parameter	**Filtered air**	**DECe (gas-phase)**	**DECe (low concentration)**	**DECe (high concentration)**
4-Week DECe exposure				
PM mass, TEOM ($\mu g/m^3$)	1.4 ± 0.1	30.1 ± 7.1	68.4 ± 6.1	988.6 ± 54.4
O_2 (%)	21.0 ± 0.2	20.1 ± 0.4	21.1 ± 0.3	20.0 ± 0.4
CO (ppm)	0.3 ± 0.2	44.3 ± 10.7	3.2 ± 0.6	42.6 ± 15.0
NO (ppm)	0.4 ± 0.3	37.5 ± 4.3	2.8 ± 0.8	35.3 ± 9.8
NO_2 (ppm)	0.6 ± 0.5	5.6 ± 1.1	0.7 ± 0.3	4.0 ± 1.5
Temperature (°F)	73.6 ± 1.0	72.6 ± 0.5	73.9 ± 0.6	72.1 ± 0.9
RH (%)	44.0 ± 5.1	49.5 ± 3.1	51.5 ± 4.3	36.0 ± 0.9

Each value in the table represents the average ± SD of the mean daily values for each exposure day.
Abbreviations: DE, diesel exhaust; DECe, cerium oxide nanoparticles added to diesel fuel; PM, particulate matter; TEOM, tapered element oscillating microbalance; RH, relative humidity.

22 and 50 nm. While the HEPA filter effectively reduced particle concentrations, similar levels of all gases were reported for the high concentration and gas-phase chambers for both the 2-day and 4-week exposures (Table 1). XRF analysis of the chamber filters indicated that Ce additive at 10 ppm concentration resulted in a final Ce content that was 0.4% and 0.9% of the total PM mass for the low concentration and high concentration of DECe, respectively.

Deposition of Ce in the Lung and Liver after Exposure to DECe

Analysis of lung and liver tissue in rats exposed to DECe resulted in concentration- and time-dependent increases in Ce content. The lung levels of Ce in rats exposed to the high concentration were more than 10-fold greater than the levels achieved at the low concentration for both the 2-day and 4-week exposure time points (Fig. 2A). The 4-week exposure resulted in accumulation of Ce in the lung at nearly four times the levels observed following the 2-day exposure (Fig. 2B). There was no significant increase in liver Ce levels at the 2-day exposure with either concentration; however, increases in liver cerium levels were noted at both the low and high concentrations at the 4-week time point (Fig. 2C). The 4-week exposure to the high concentration of DECe resulted in over six times the Ce deposition in the liver when compared with exposure at the low concentration (Fig. 2D). In addition, when the rats exposed to filtered air or high concentration of DECe were allowed a 14-day recovery period following the 4-week exposure, a 35% reduction in lung levels and 59% reduction in liver levels of Ce occurred (Fig. 2B and 2D). Collectively, these data suggest accumulation of Ce in the lung and liver resulting from an extended exposure period, followed by a delayed clearance over time.

The MPPD model was used to estimate the fraction of particles deposited in the total lung (d_f) in animals exposed to the low and high concentrations of DECe for either 2 days or 4 weeks (Table 2). Based on the MPPD model predictions, the estimated pulmonary deposition of total PM (D_{PM}) and Ce (D_{Ce}) was calculated. These predicted Ce levels were compared with the measured lung levels of Ce (Fig. 2A) to estimate the percent of Ce retained in the lungs (Table 2). Exposure to the low concentration of DECe resulted in a greater percent of Ce retained in the lungs as compared with exposure to the high concentration at both the 2-day (122% vs 56%, respectively) and 4-week time point (40% vs 22%, respectively), indicating inefficient clearance of Ce at the low concentration.

Lung Injury and Inflammation Following Exposure to DE and DECe

In the comparative study examining the 2-day exposure to the high concentration of DE and DECe in parallel, BALF NAG activity, a marker for macrophage activation, was increased significantly in rats exposed to DECe but not DE (Fig. 3A). There were also marginal but not statistically significant increases in the levels of several other markers of lung injury (Fig. 3B–D) and inflammation (Fig. 3E and 3F), with DECe resulting in consistently greater values compared with DE. As the DECe chamber achieved 20% less PM

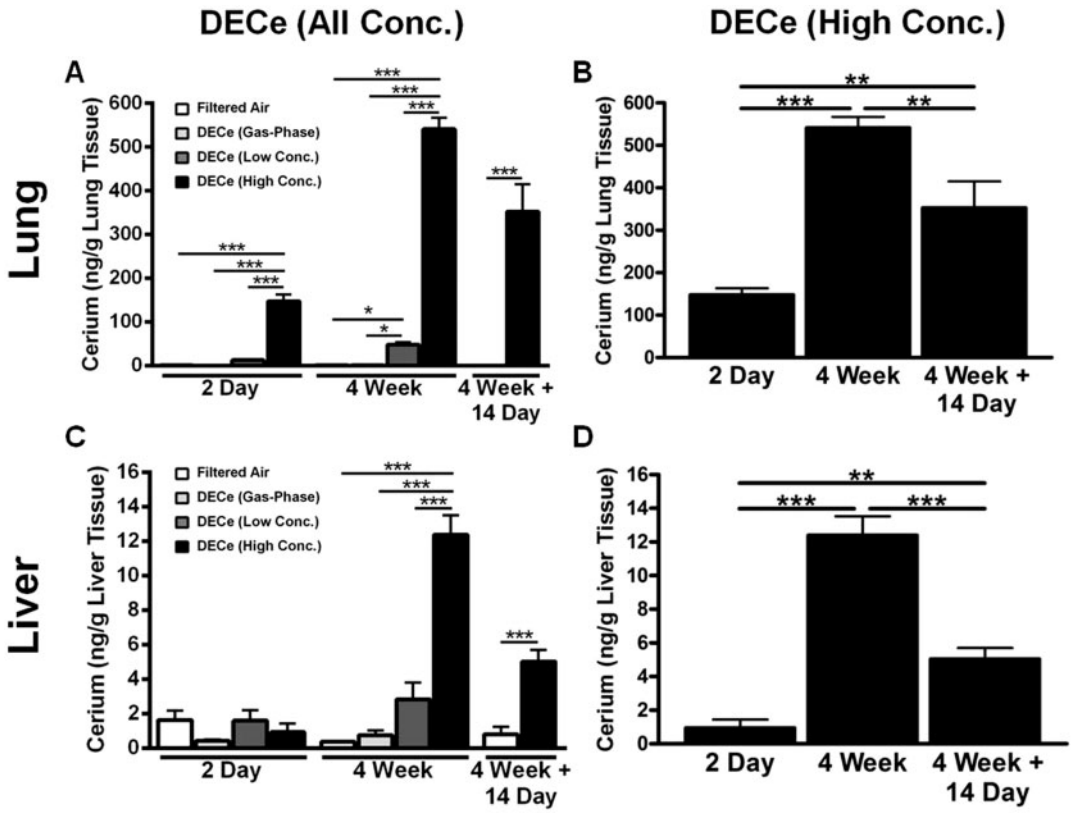

FIG. 2. Concentration- and time-dependent accumulation of Ce in the lungs and livers of rats inhaling DE with Ce additive. Ce levels following exposure to filtered air or DECe (gas-phase, low concentration, or high concentration) for 2 days, 4 weeks, or 4 weeks with a 14-day recovery period were analyzed in the A, B, lung and C, D, liver by inductively coupled plasma-mass spectrometry. B and D, Ce levels following exposure to the high concentration of DECe were compared at the different time points. Data show mean ± SE of $n = 8$ rats per group. $^{*}p < .05$; $^{**}p < .01$; $^{***}p < .001$ significantly different from other groups.

TABLE 2. Estimated Pulmonary Deposition of PM and Ce

DECe	Length of exposure	PM mass ($\mu g/m^3$)	MMAD	d_f	Estimated D_{PM} ($\mu g/g$ lung tissue)[a]	P_{Ce} (%)	Estimated D_{Ce} (ng/g lung tissue)[a]	Measured lung Ce levels (ng/g lung tissue)	Estimated lung retention of Ce (%)
Low concentration	2 Days	66.4	31	0.290	3.0	0.36	10.8	13.2	122.2
	4 Weeks	68.4	31	0.290	30.9	0.39	120.7	48.5	40.2
High concentration	2 Days	1003.5	79	0.189	29.6	0.89	263.3	148.0	56.2
	4 Weeks	988.6	79	0.189	291.4	0.85	2477.6	541.3	21.8

[a]An estimated lung weight of 2.0 g for 12-week-old male Sprague Dawley rats was used to convert total lung deposition to per unit weight (Piao *et al.*, 2013).
Abbreviations: MMAD, mass median aerodynamic diameter; d_f, pulmonary deposition fraction for the total lung as predicted by the MPPD model; D_{PM}, pulmonary deposition of PM in the total lung; P_{Ce}, percent of Ce present in PM; D_{Ce}, pulmonary deposition of Ce in the total lung.

mass concentration than the DE chamber (Table 1), this suggests that the effects induced by DECe were underestimated and that DECe on an equal mass basis is more likely to induce greater lung injury and inflammation than DE alone.

The 2-day and 4-week exposure studies with DECe consisted of rats exposed to a low concentration, high concentration, and gas-phase components from the high concentration. BALF total protein and albumin, markers of lung permeability, were significantly increased in rats following a 2-day exposure to only the gas-phase components of DECe (Fig. 4A and 4B). GGT activity levels, a marker of lung cell injury, were significantly increased in BALF from rats exposed to the high concentration and gas-phase components of DECe at the 2-day and 4-week time points (Fig. 4C). BALF neutrophils were significantly increased following a 2-day exposure to the high concentration and gas-phase components of DECe (Fig. 4D). No significant changes in BALF alveolar macrophage (Fig. 4E), LDH, or NAG activity levels (data not shown) were noted. These data indicate that the acute pulmonary injury and inflammation following exposure to the whole exhaust are likely to be driven by the gas-phase components of DECe.

Histological and Ultrastructural Lung Effects of DE and DECe Exposure

Lungs were examined by light microscopy to evaluate the effects of exposure to the high concentration of DE and DECe. Two exposure-related findings were apparent in comparison to the control lung sample (Fig. 5A): (1) minimal to mild yellow-brown to black pigmentation within the alveolar macrophages following a 2-day exposure to DE and DECe (data not shown)

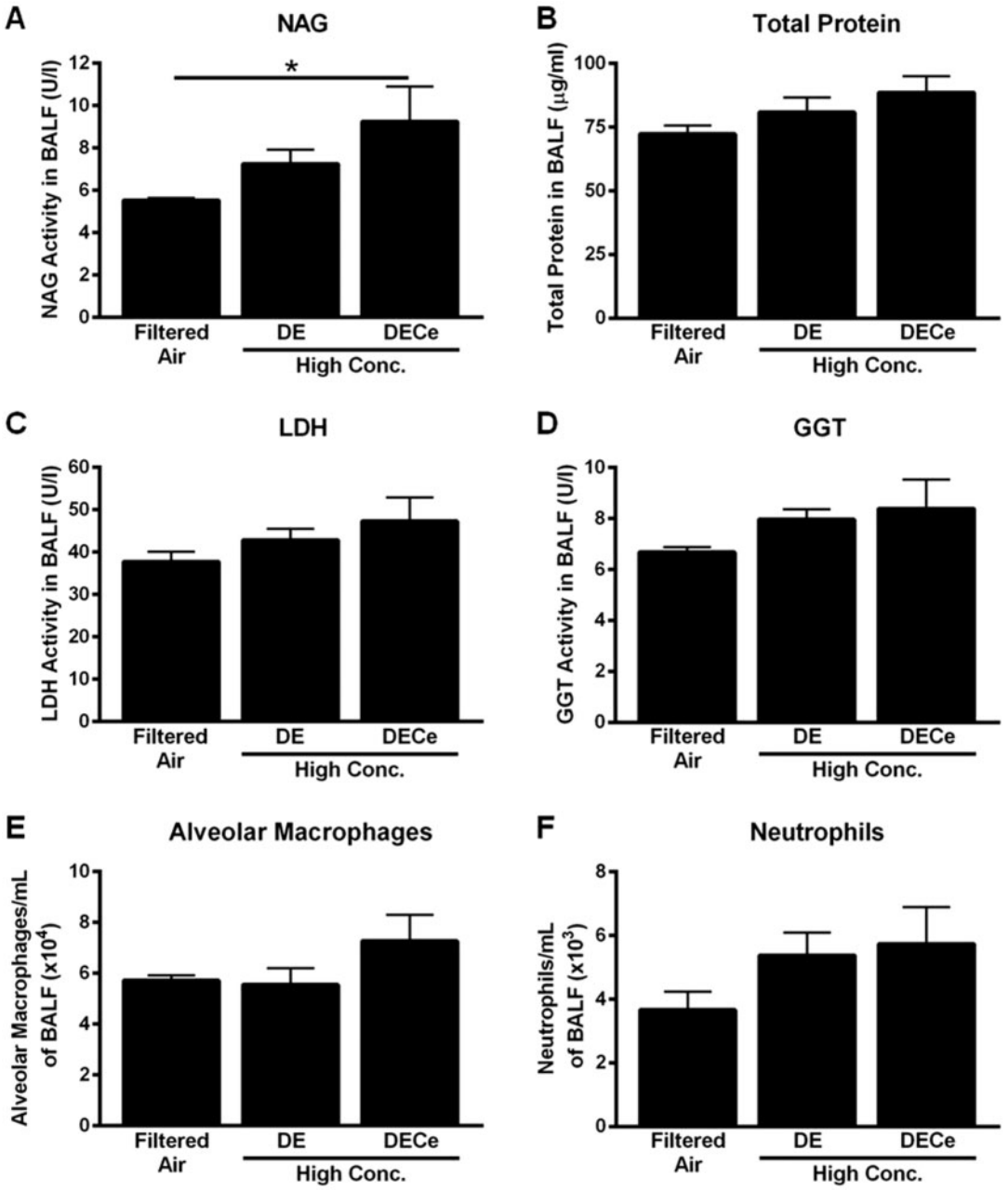

FIG. 3. Comparative effect of DE and DECe exposures on lung injury markers and inflammation. Rats were exposed to filtered air, DE, or DECe for two consecutive days. Bronchoalveolar lavage fluid (BALF) samples were collected 1 day after final exposure and analyzed for A, N-acetyl glucosaminidase (NAG) activity, B, total protein, C, lactate dehydrogenase (LDH) activity, D, γ-glutamyl transferase (GGT) activity, E, alveolar macrophages, and F, neutrophils. Data show mean ± SE of $n = 6$ rats/group. *$p < .05$ significantly different from other groups.

and 4-week exposure to DECe (Fig. 5B); and (2) minimal increase in alveolar macrophages (histiocytosis) following exposure to DECe at 4 weeks with and without a 14-day recovery period (Fig. 5C and 5D). The alveolar histiocytosis was characterized by slightly increased numbers of alveolar macrophages that in general were diffusely distributed throughout the lung. The pigmented particles found in the alveolar macrophages from the recovery animals were more commonly observed in punctate aggregates, possibly reflecting continued cellular processing of the material (Fig. 5D). No effects of the gas-phase exposure were observed (data not shown).

Pulmonary changes were examined by TEM following exposure to filtered air or high concentration of DECe for 4 weeks (Fig. 6A–D). Intracytoplasmic foreign material was observed within alveolar macrophages from DECe (Fig. 6C) but not control (Fig. 6A) lungs. This material was characterized by numerous smooth electron dense bodies ranging in size from 10 to 600 nm within membrane bound organelles, in some cases containing variably sized clear spaces. Intracellular edema was also present in alveolar macrophages following exposure to DECe as indicated by increased clear space within the cytoplasm (Fig. 6C). Enlarged alveolar septal capillaries, often with neutrophils, were present within the capillary lumens from DECe lungs (Fig. 6D) compared with control (Fig. 6B). Adjacent septal and capillary membranes were separated by increased clear space, indicating edema (Fig. 6D). Animals that were allowed

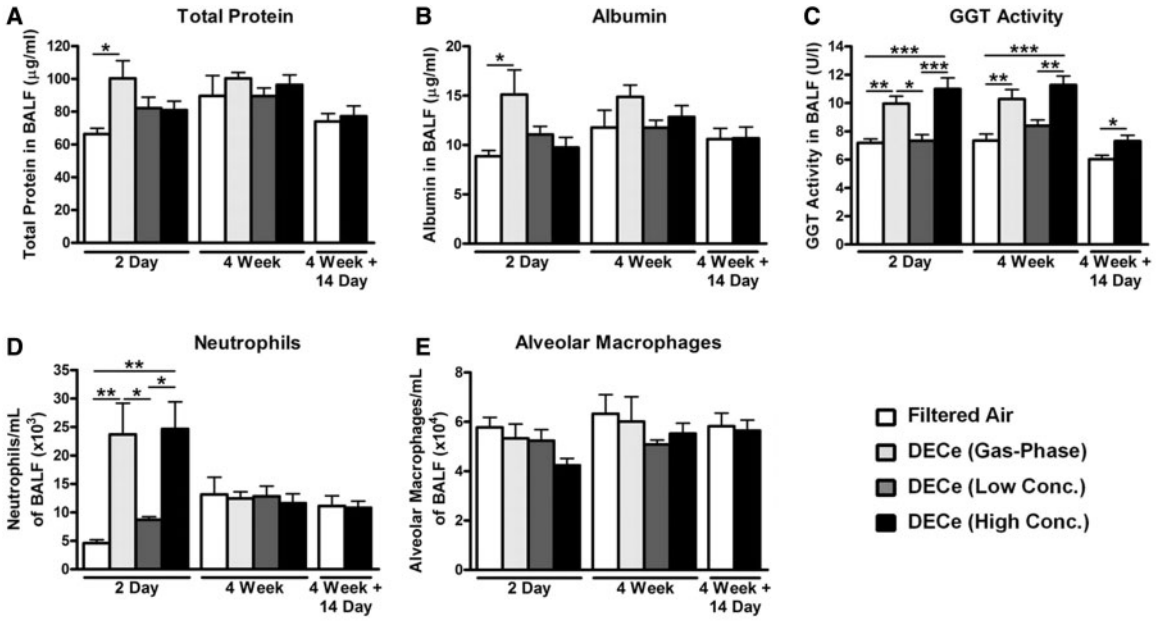

FIG. 4. Acute and long-term effect of DECe exposures on lung injury markers and inflammation. Rats were exposed to filtered air or DECe (gas-phase, low concentration, or high concentration) for 2 days, 4 weeks, or 4 weeks with a 14-day recovery period. Bronchoalveolar lavage fluid (BALF) samples were collected 1 day after final exposure or recovery period and analyzed for A, total protein, B, albumin, C, GGT activity, D, neutrophils, and E, alveolar macrophages. Data show mean ± SE of $n = 8$ rats/group. $^{*}p < .05$; $^{**}p < .01$; $^{***}p < .001$ significantly different from other groups.

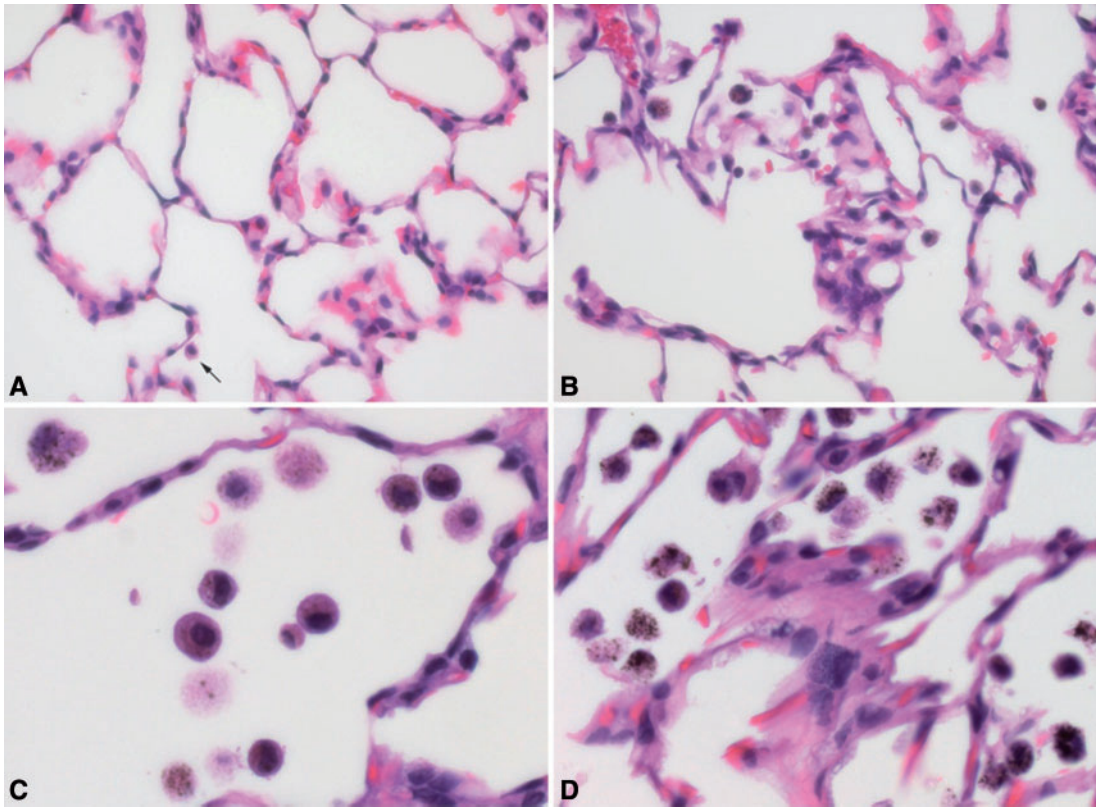

FIG. 5. Histopathological effects in the lung following exposure to DECe. A, Control animal exposed to filtered air for 4 weeks: Normal alveolar air spaces and septa. Air spaces contain scattered pulmonary interstitial macrophages (arrow). B, Rat exposed to DECe (high concentration) for 4 weeks: Alveolar air spaces contain increased numbers of macrophages with minimal to mild pigmentation. C, Rat exposed to DECe (high concentration) for 4 weeks: Higher magnification view of pulmonary alveolar macrophages containing dark yellow to black intracytoplasmic pigments. D, Rat exposed to DECe (high concentration) for 4 weeks with a 14-day recovery: Increased numbers of pulmonary alveolar macrophages containing intracytoplasmic pigment. Images were taken at an objective magnification of ×40 (A, B) or ×60 (C, D).

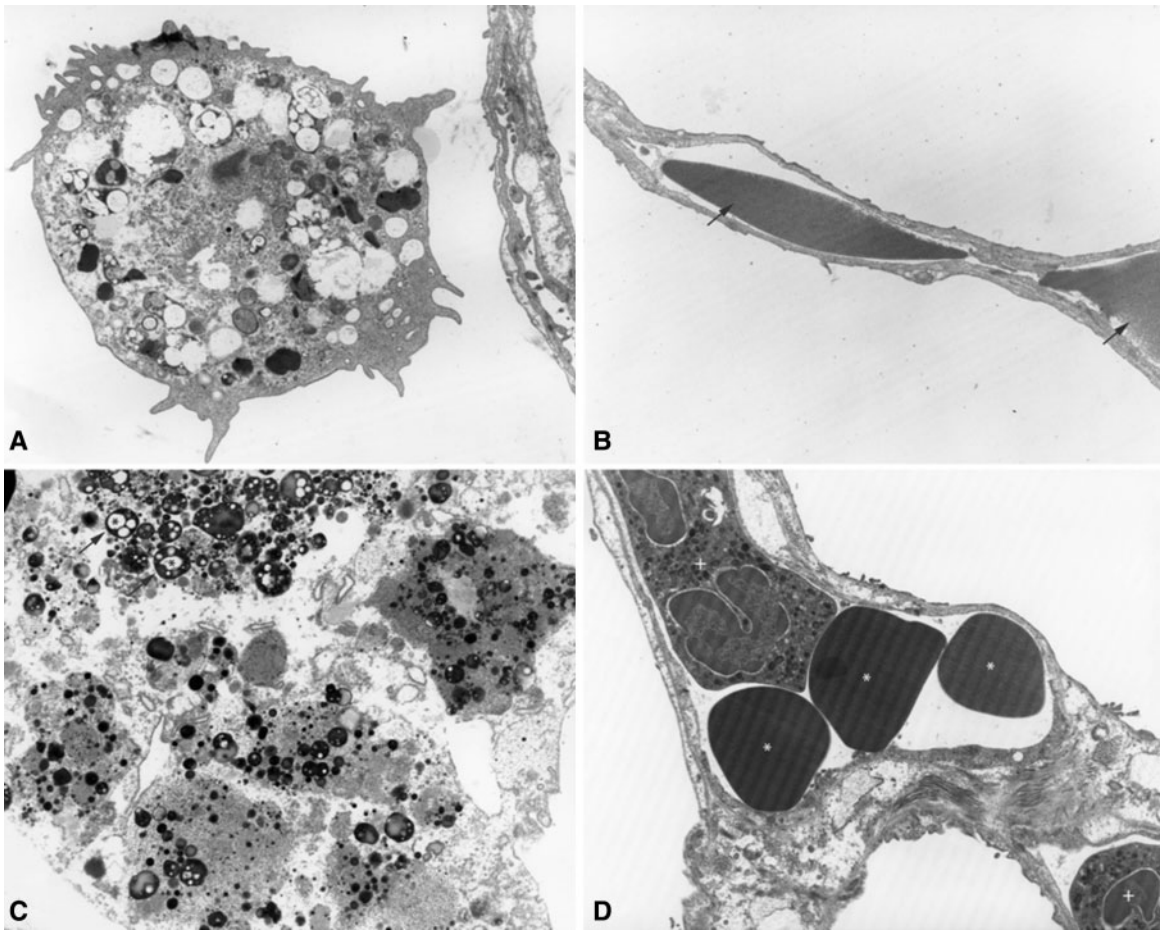

FIG. 6. Pulmonary changes on transmission electron microscopy following exposure to DECe. A, Control rat exposed to filtered air for 4 weeks: A normal pulmonary interstitial macrophage with several intracytoplasmic primary and secondary lysosomal vacuoles of varying electron density present. B, Control animal exposed to filtered air for 4 weeks: A normal alveolar septal capillary. Two elliptical erythrocytes are present within the capillary lumen (arrows). C, Rat exposed to DECe (high concentration) for 4 weeks: A pulmonary alveolar macrophage containing possible intracytoplasmic foreign material. The cytoplasm is filled with multiple smooth electron dense bodies ranging in size from 10 to 600 nm within membrane bound organelles (arrows). Multiple clear spaces appear within the foreign material (*). Increased clear space within the cytoplasm indicates intracellular edema. D, Rat exposed to DECe (high concentration) for 4 weeks: An enlarged alveolar septal capillary. Three erythrocytes (*) and two neutrophils (+) are present within the capillary lumen. Adjacent septal and capillary membranes are separated by increased clear space, indicating edema. Images were taken at a magnification of ×15 400 (A, B, D) or ×22 200 (C).

TABLE 3. Changes in Aortic RNA for Markers of Vasoconstriction, Thrombosis, Inflammation, and Atherogenesis in Rats Exposed to DECe for 4 weeks

Marker	Filtered air	DECe (gas-phase)	DECe (low concentration)	DECe (high concentration)
eNOS	1.05 ± 0.15	1.98 ± 0.25	2.18 ± 0.39*	2.24 ± 0.31*
ET-1	1.12 ± 0.23	1.33 ± 0.16	1.57 ± 0.14	1.47 ± 0.15
ETRB	1.19 ± 0.33	1.73 ± 0.36	1.88 ± 0.23	1.58 ± 0.37
tPA	1.05 ± 0.13	1.58 ± 0.20	1.41 ± 0.15	1.23 ± 0.09
PAI-1	1.18 ± 0.35	0.92 ± 0.20	2.88 ± 0.78	1.08 ± 0.32
TF	1.04 ± 0.11	1.72 ± 0.17**	1.52 ± 0.10	1.64 ± 0.17*
TNF-α	1.17 ± 0.29	2.15 ± 0.09*	2.43 ± 0.18**	1.84 ± 0.25
ATR1	1.10 ± 0.22	1.75 ± 0.34	1.87 ± 0.47	1.84 ± 0.33
Caveolin-1	1.04 ± 0.12	1.13 ± 0.07	1.01 ± 0.06	1.25 ± 0.10

Values are calculated as relative fold change over filtered air exposed controls after normalizing the expression with Hprt1. Values represent mean ± SE of six rat tissues, each analyzed in duplicate.

*$p < .05$, **$p < .01$ significantly different than filtered air.

Abbreviations: eNOS, endothelial nitric oxide synthase; ET-1, endothelin-1; ETRB, endothelin receptor B; tPA, tissue plasminogen activator; PAI-1, plasminogen activator inhibitor-1; TF, tissue factor; TNF-α, tumor necrosis factor-α; ATR1, angiotensin receptor type 1 a.

the 14-day recovery period following the 4-week exposure did not show improvement in the incidence or severity of alveolar histiocytosis (data not shown).

Systemic Effects of Inhaled DECe

In general, the CBC encompassing changes in hematological parameters, platelets, and white blood cell profiles showed minimal exposure related changes (data not shown). ADP-induced platelet aggregation determined *in vitro* was also not significantly affected with exposure to DECe (gas-phase, low concentration, and high concentration; data not shown). Relatively small changes were noted in aortic RNA for markers of vascular activity, thrombosis, inflammation, and atherogenesis in rats exposed for 4 weeks to DECe (Table 3). Specifically, expression of endothelial nitric oxide synthase, tissue factor, and tumor necrosis factor-α were significantly increased, suggesting that exposure to whole DECe exhaust or gas-phase components of DECe may contribute to vascular contractility changes, procoagulant responses, and inflammation.

DISCUSSION

Health consequences of soot emissions from diesel fueled engines with CeO_2 nanoparticle additive may differ greatly from those that occur in the absence of a Ce fuel borne catalyst. The rise in use of this fuel additive will lead to increased environmental deposition of Ce, which raises concerns about potential long-term health consequences (HEI, 2001). More importantly, the addition of a Ce catalyst results not only in overall PM mass reductions but also a modified exhaust chemistry (Zhang *et al.*, 2013). This change in chemistry and the possibility of Ce accumulation in the body over a lifetime of exposure warrants examination of potential adverse health effects from an altered emission profile. Few studies have undertaken examination of health consequences following exposure to DECe exhaust, and detailed evaluation in healthy animal models is lacking (Cassee *et al.*, 2012; HEI, 2001; Ma *et al.*, 2014). In this study, we undertook extensive toxicological analysis of laboratory generated exhausts of diesel with or without CeO_2 nanoparticle fuel additive.

In the first acute study comparing DE and DECe in parallel, we demonstrated that DECe caused a greater increase in BALF NAG activity (a marker for macrophage activation) than DE. Although not significant with other markers of lung injury and inflammation, this pattern was consistently observed and occurred despite 20% less mass concentration in the DECe chamber compared with the DE chamber. These findings suggest that DECe exposure might induce greater pulmonary injury upon acute inhalation, providing support for a recent study that demonstrated increased and sustained pulmonary damage in rats intratracheally instilled with diesel particles containing CeO_2 nanoparticles compared to diesel particles alone (Ma *et al.*, 2014). These data are at odds with the results from another study which implied that the addition of a Ce-based fuel borne catalyst may reduce the atherosclerotic burden associated with exposure to diesel fuel (Cassee *et al.*, 2012). Collectively, these studies indicate that additional investigations must be conducted comparing DE and DECe exposure in healthy and compromised animal models to fully understand the health risk involved with adding CeO_2 nanoparticles to diesel fuel.

In our second study, we examined pulmonary and systemic health outcomes in addition to analysis of Ce tissue deposition following acute and subacute exposure to whole DECe or gas-phase components in healthy rats. The augmented effects on albumin and total protein following a 2-day exposure to high concentration and gas-phase components of DECe were not evident in rats exposed for 4 weeks; however, the increases in BALF GGT activity (a marker for lung cell injury) were sustained, suggesting that the effect of whole exhaust and gas-phase components on GGT activity was not reversible over a 4-week period. Significant increases in BALF neutrophils with DECe (high concentration and gas-phase components) were evident in rats exposed for 2 days but not 4 weeks, suggesting that the neutrophilic inflammatory response was acute and that a blunting of the response occurs with repeated exposure to DECe. This latter finding differs from other high concentration metal-rich oil-combustion PM studies where progressive inflammation was observed upon repeated exposure (Kodavanti *et al.*, 2002).

Light and transmission electron microscopy examination provided further insights into the morphologic effects of inhaled DECe in the lung. Ultrastructural changes included interstitial neutrophils and edema, consistent with increased neutrophils in BALF observed following a 2-day DECe exposure and the continued increases in BALF GGT activity. The increased number of alveolar macrophages and presence of pigmentation was similar between the animals exposed to DE and DECe for 2 days, which corresponds to the findings of Cassee *et al.* (2012) who observed a comparable response in an atherosclerosis-prone mouse model. Notably, the alveolar histiocytosis, edema, and presence of pigmented particles within the alveolar macrophages seen at 4 weeks were still apparent after a 14-day recovery period following exposure to DECe. It is likely that alterations of the diesel soot particles with CeO_2 nanoparticle additive may contribute to less efficient clearing from the lung. This would align with recent studies that have demonstrated a long elimination half-life and accumulation of Ce in the lungs following exposure to CeO_2 nanoparticles (Geraets *et al.*, 2012; He *et al.*, 2010).

The high concentration of DECe exhaust contains CO, NO_x, and other organic vapors at environmentally relevant concentrations that may contribute to observed health effects in different ways. Therefore, we wanted to determine the relative contribution of gas-phase components in the whole exhaust. Many of the adverse pulmonary effects as determined by BALF analysis of DECe at this concentration were also observed following filtration of the particles from the exhaust, indicating that the contribution of gas-phase components cannot be ignored. These data correspond with a previous study that demonstrated acute pulmonary injury and inflammation in normotensive and hypertensive rats following exposure to the gas-phase components of DE (Kodavanti *et al.*, 2013). CO and NO are known to have many biological effects including the ability to induce vasorelaxation (Cooke and Dzau, 1997; Leffler *et al.*, 2011). Following exposure, these components could reach alveolar capillaries where they can directly impact the microvasculature contractility. Often these effects are opposite of those expected from DE (Li *et al.*, 2005; Peretz *et al.*, 2008), which could lead to underestimation of some adverse health outcomes observed with whole exhaust. We observed that only the gas-phase components induced pulmonary vascular protein leakage whereas markers of pulmonary inflammation and lung epithelial cell injury were noted with both gas-phase and high concentration of DECe. This finding supports a previous study demonstrating increased BALF neutrophils and GGT activity levels following a 2-day and 4-week exposure to gas-phase and whole DE in Wistar-Kyoto rats (Gordon *et al.*, 2012). Although an earlier study from our laboratory illustrated that bulk collected diesel particles without gas-phase components induced lung injury in rats (Kodavanti *et al.*, 2011), this current data indicates

that one cannot conclude that the lung injury resulting from such exhausts are attributed to just soot particles. Partitioning of the gas-phase volatile organic substances on soot particles during exhaust generation and bulk particle collection may contribute to the toxicity of bulk collected DE particles, but separating these attributes will be technically challenging.

The addition of CeO_2 nanoparticles to diesel fuel has been shown to alter the emission profile and increase the number of ultrafine particles emitted (Zhang *et al.*, 2013). Our results support this observation and, in addition, demonstrate that soot particles were of smaller diameter at the low concentration when the dilution factor was increased. Systemic translocation of smaller particles has been shown to be greater than larger particles (Sadauskas *et al.*, 2009), which could potentially result in increased systemic translocation of particles at our low concentration. Examination of health consequences indicated that the lung injury caused by exposure to the low concentration was minimal relative to injury caused by the high concentration; however, we noted that aortic markers of vascular activity and inflammation were affected similarly by both. The estimated percent of Ce retained in the lung was greater following exposure to the low concentration of DECe when the particle diameter range was smaller, indicating that Ce is not as efficiently cleared when animals are exposed to an increased number of ultrafine particles. Adverse vascular responses of diesel and gasoline exhausts have been noted to occur in atherosclerosis-prone mice exposed to low concentrations similar to what is used in our present study (Campen *et al.*, 2010). Our results extend these observations by demonstrating effects on vascular markers in a healthy animal model. At the low concentration of DECe, the gas-phase components are below the levels where systemic impacts are expected (Hesterberg *et al.*, 2009a; WHO, 2010). Thus, the vascular effects of low concentration exhaust emissions may be attributed to the DECe ultrafine particles that have the propensity to translocate systemically. These results suggest that vascular outcomes at the low concentration of DECe exposure are possible and warrant further examination, including chronic exposures in healthy and compromised rodent models.

One of the ancillary objectives of this work was to examine tissue Ce burden and clearance in rats inhaling DECe, especially as Ce has been detected in the blood from residents of Europe where this additive is used as a diesel catalyst (Hollriegl *et al.*, 2010). Extrapulmonary translocation and accumulation of Ce occurs in various organs following a subacute inhalation exposure to CeO_2 nanoparticles in rats (Geraets *et al.*, 2012). Our data correspond with this observation and extend it to illustrate a concentration- and time-dependent accumulation of Ce in lung and liver tissue following exposure to DECe. He *et al.* (2010) have shown that CeO_2 nanoparticles have an elimination half-life from the lung of 103 days after a single high concentration exposure via intratracheal instillation. Accordingly, our data indicate a delayed clearance of Ce from these tissues as demonstrated by the small percent that was cleared from the organs in the rats given a 14-day recovery period. Furthermore, the low levels of Ce present in the liver following the 2-day exposure suggest a delay in biodistribution as the Ce is cleared from the lung. Intratracheal instillation of CeO_2 nanoparticles has been shown to induce hydropic degeneration of hepatocytes, dilate the sinusoids, and elevate several serum markers of hepatic toxicity (Nalabotu *et al.*, 2011), suggesting that Ce accumulation in the liver following DECe exposure might induce liver toxicity and will need to be considered in future studies. When theoretical lung Ce burden was calculated by imputing real exposure values and ventilatory parameters into the MPPD model, which did not take into account clearance, and compared to actual lung Ce concentrations, it was apparent that Ce was cleared slowly from the lung over time. Thus, the health consequences of Ce retained in the lung along with soot particle clearance will need to be investigated further.

Our study design has a few limitations. The mass concentrations of DE and DECe used in this study are several fold higher than ambient exposure levels. However, tailpipe emissions and near roadway levels of DE can reach mass concentrations in the hundreds of $\mu g/m^3$ PM (Buzzard *et al.*, 2009). The low concentration of DECe used in our study is likely to occur near roadways and is more realistic for human exposure. In addition, we found that the low concentration of DECe preserved a bimodal PSD and decreased the median diameter of the particles being emitted. This allowed us to examine the systemic effects of increased ultrafine particle number. The high concentration of DECe, which can occur during an occupational exposure (Stayner *et al.*, 1998), was used to increase the likelihood of finding detectable changes in lung injury biomarkers. In a previous study using an iron fuel borne catalyst, Nash *et al.* (2013) describe that the metal catalyst particles undergo complex processes where they are incorporated into soot during its formation, enhance soot oxidation within the flame, are liberated from the receding carbon matrix, and continue to interact via coagulation and agglomeration with each other and residual soot particles post flame. In the exhaust, these metal catalyst particles can be incorporated within, deposited externally upon, or remain independent of the diesel soot particles producing a bimodal PSD. Depending on dilution, this bimodal PSD eventually evolves into a single accumulation mode, but high dilution rates, characteristic of highway environments, can preserve this bimodal PSD for tens of minutes. This is an important area to research further because the rates of deposition, absorption, translocation, and elimination might differ between CeO_2 nanoparticles and diesel soot particles, which may affect the location and severity of lung and systemic injury.

In conclusion, we report that inhalation exposures to DECe are likely to have greater adverse pulmonary effects than DE alone. We observed that the particle-free gas-phase components of DECe, in addition to the whole exhaust, were capable of inducing pulmonary damage. DECe is also likely to impair deep lung alveolar integrity upon chronic exposure with little recovery upon termination of exposure. Finally, we have demonstrated that significant quantities of Ce accumulate in the lung and translocate to the liver with delayed clearance, leading to increased systemic Ce burden and potential pathological effects. These novel findings add to the limited data available concerning exposure to DECe, and suggest that the pulmonary and systemic health consequences of Ce additive to diesel fuel should be further evaluated.

FUNDING

This work was supported by the U.S. Environmental Protection Agency/University of North Carolina Toxicology Training Agreement CR835152010 to S.J.S.; U.S. Environmental Protection Agency Senior Environmental Employment Program to R.F.T.; and the Division of the National Toxicology Program of the National Institutes of Health.

ACKNOWLEDGMENTS

The authors would like to thank Drs William Boyes and Kevin Dreher of the U.S. EPA for their critical review of this

manuscript. The contributing authors declare no competing financial interests or other conflicts of interest.

REFERENCES

Brunekreef, B., and Holgate, S. T. (2002). Air pollution and health. *Lancet* **360,** 1233–1242.

Buzzard, N. A., Clark, N. N., and Guffey, S. E. (2009). Investigation into pedestrian exposure to near-vehicle exhaust emissions. *Environ. Health* **8,** 13.

Campen, M. J., Babu, N. S., Helms, G. A., Pett, S., Wernly, J., Mehran, R., and McDonald, J. D. (2005). Nonparticulate components of diesel exhaust promote constriction in coronary arteries from ApoE-/- mice. *Toxicol. Sci.* **88,** 95–102.

Campen, M. J., Lund, A. K., Doyle-Eisele, M. L., McDonald, J. D., Knuckles, T. L., Rohr, A. C., Knipping, E. M., and Mauderly, J. L. (2010). A comparison of vascular effects from complex and individual air pollutants indicates a role for monoxide gases and volatile hydrocarbons. *Environ. Health Perspect.* **118,** 921–927.

Cassee, F. R., Campbell, A., Boere, A. J., McLean, S. G., Duffin, R., Krystek, P., Gosens, I., and Miller, M. R. (2012). The biological effects of subacute inhalation of diesel exhaust following addition of cerium oxide nanoparticles in atherosclerosis-prone mice. *Environ. Res.* **115,** 1–10.

Cassee, F. R., van Balen, E. C., Singh, C., Green, D., Muijser, H., Weinstein, J., and Dreher, K. (2011). Exposure, health and ecological effects review of engineered nanoscale cerium and cerium oxide associated with its use as a fuel additive. *Crit. Rev. Toxicol.* **41,** 213–229.

Chen, S., Hou, Y., Cheng, G., Zhang, C., Wang, S., and Zhang, J. (2013). Cerium oxide nanoparticles protect endothelial cells from apoptosis induced by oxidative stress. *Biol. Trace Elem. Res.* **154,** 156–166.

Cooke, J. P., and Dzau, V. J. (1997). Nitric oxide synthase: Role in the genesis of vascular disease. *Annu. Rev. Med.* **48,** 489–509.

Cosselman, K. E., Krishnan, R. M., Oron, A. P., Jansen, K., Peretz, A., Sullivan, J. H., Larson, T. V., and Kaufman, J. D. (2012). Blood pressure response to controlled diesel exhaust exposure in human subjects. *Hypertension* **59,** 943–948.

Eom, H. J., and Choi, J. (2009). Oxidative stress of CeO2 nanoparticles via p38-Nrf-2 signaling pathway in human bronchial epithelial cell, BEAS-2B. *Toxicol. Lett.* **187,** 77–83.

EPA. (1994). *Method 200.8 Revision 5.4: Determination of Metals and Trace Elements in Water and Wastes by Inductively Coupled Plasma - Mass Spectrometry*. Available at: http://water.Epa.Gov/scitech/methods/cwa/bioindicators/upload/2007_07_10_methods_method_200_8.Pdf. Accessed October 8, 2014.

EPA. (1997). *Compendium Method IO-3.3: Determination of Metals in Ambient Particulate Matter Using X-ray Fluorescence (XRF) Spectroscopy*. Available at: http://www.epa.gov/ttnamti1/files/ambient/inorganic/iocompen.pdf. Accessed October 8, 2014.

Fall, M., Guerbet, M., Park, B., Gouriou, F., Dionnet, F., and Morin, J. P. (2007). Evaluation of cerium oxide and cerium oxide based fuel additive safety on organotypic cultures of lung slices. *Nanotoxicology* **1,** 227–234.

Geraets, L., Oomen, A. G., Schroeter, J. D., Coleman, V. A., and Cassee, F. R. (2012). Tissue distribution of inhaled micro- and nano-sized cerium oxide particles in rats: Results from a 28-day exposure study. *Toxicol. Sci.* **127,** 463–473.

Ghio, A. J., Sobus, J. R., Pleil, J. D., and Madden, M. C. (2012). Controlled human exposures to diesel exhaust. *Swiss. Med. Wkly.* **142,** w13597.

Gojova, A., Lee, J. T., Jung, H. S., Guo, B., Barakat, A. I., and Kennedy, I. M. (2009). Effect of cerium oxide nanoparticles on inflammation in vascular endothelial cells. *Inhal. Toxicol.* **21**(Suppl. 1)**,** 123–130.

Gordon, C. J., Jarema, K. A., Lehmann, J. R., Ledbetter, A. D., Schladweiler, M. C., Schmid, J. E., Ward, W. O., Kodavanti, U. P., Nyska, A., and MacPhail, R. C. (2013). Susceptibility of adult and senescent brown norway rats to repeated ozone exposure: An assessment of behavior, serum biochemistry and cardiopulmonary function. *Inhal. Toxicol.* **25,** 141–159.

Gordon, C. J., Schladweiler, M. C., Krantz, T., King, C., and Kodavanti, U. P. (2012). Cardiovascular and thermoregulatory responses of unrestrained rats exposed to filtered or unfiltered diesel exhaust. *Inhal. Toxicol.* **24,** 296–309.

Gowdy, K. M., Krantz, Q. T., King, C., Boykin, E., Jaspers, I., Linak, W. P., and Gilmour, M. I. (2010). Role of oxidative stress on diesel-enhanced influenza infection in mice. *Part. Fibre Toxicol.* **7,** 34.

He, X., Zhang, H., Ma, Y., Bai, W., Zhang, Z., Lu, K., Ding, Y., Zhao, Y., and Chai, Z. (2010). Lung deposition and extrapulmonary translocation of nano-ceria after intratracheal instillation. *Nanotechnology* **21,** 285103.

Health Effects Institute (HEI). (2001). Evaluation of human health risk from cerium added to diesel fuel. *Health Effects Institute Communication*, p. 9. Available at: http://pubs.healtheffects.org/view.php?id=172. Accessed October 8, 2014.

Hesterberg, T. W., Bunn, W. B., McClellan, R. O., Hamade, A. K., Long, C. M., and Valberg, P. A. (2009a). Critical review of the human data on short-term nitrogen dioxide (NO2) exposures: Evidence for NO2 no-effect levels. *Crit. Rev. Toxicol.* **39,** 743–781.

Hesterberg, T. W., Long, C. M., Bunn, W. B., Sax, S. N., Lapin, C. A., and Valberg, P. A. (2009b). Non-cancer health effects of diesel exhaust: A critical assessment of recent human and animal toxicological literature. *Crit. Rev. Toxicol.* **39,** 195–227.

Hirst, S. M., Karakoti, A., Singh, S., Self, W., Tyler, R., Seal, S., and Reilly, C. M. (2013). Bio-distribution and in vivo antioxidant effects of cerium oxide nanoparticles in mice. *Environ. Toxicol.* **28,** 107–118.

Hirst, S. M., Karakoti, A. S., Tyler, R. D., Sriranganathan, N., Seal, S., and Reilly, C. M. (2009). Anti-inflammatory properties of cerium oxide nanoparticles. *Small* **5,** 2848–2856.

Hollriegl, V., Gonzalez-Estecha, M., Trasobares, E. M., Giussani, A., Oeh, U., Herraiz, M. A., and Michalke, B. (2010). Measurement of cerium in human breast milk and blood samples. *J. Trace Elem. Med. Biol.* **24**, 193–199.

Hussain, S., Al-Nsour, F., Rice, A. B., Marshburn, J., Yingling, B., Ji, Z., Zink, J. I., Walker, N. J., and Garantziotis, S. (2012). Cerium dioxide nanoparticles induce apoptosis and autophagy in human peripheral blood monocytes. *ACS Nano.* **6,** 5820–5829.

Johnson, A. C., and Park, B. (2012). Predicting contamination by the fuel additive cerium oxide engineered nanoparticles within the united kingdom and the associated risks. *Environ. Toxicol. Chem.* **31,** 2582–2587.

Jung, H., Kittelson, D. B., and Zachariah, M. R. (2005). The influence of a cerium additive on ultrafine diesel particle emissions and kinetics of oxidation. *Combust. Flame* **142,** 276–288.

Kodavanti, U. P., Schladweiler, M. C., Ledbetter, A. D., Hauser, R., Christiani, D. C., McGee, J., Richards, J. R., and Costa, D. L. (2002). Temporal association between pulmonary and systemic effects of particulate matter in healthy and cardiovascular compromised rats. *J. Toxicol. Environ. Health A* **65,** 1545–1569.

Kodavanti, U. P., Schladweiler, M. C., Ledbetter, A. D., Ortuno, R. V., Suffia, M., Evansky, P., Richards, J. H., Jaskot, R. H., Thomas, R., Karoly, E., *et al.* (2006). The spontaneously hypertensive rat: An experimental model of sulfur dioxide-induced airways disease. *Toxicol. Sci.* **94,** 193–205.

Kodavanti, U. P., Thomas, R., Ledbetter, A. D., Schladweiler, M. C., Shannahan, J. H., Wallenborn, J. G., Lund, A. K., Campen, M. J., Butler, E. O., Gottipolu, R. R., *et al.* (2011). Vascular and cardiac impairments in rats inhaling ozone and diesel exhaust particles. *Environ. Health Perspect.* **119,** 312–318.

Kodavanti, U. P., Thomas, R. F., Ledbetter, A. D., Schladweiler, M. C., Bass, V., Krantz, Q. T., King, C., Nyska, A., Richards, J. E., Andrews, D., *et al.* (2013). Diesel exhaust induced pulmonary and cardiovascular impairment: The role of hypertension intervention. *Toxicol. Appl. Pharmacol.* **268,** 232–240.

Leffler, C. W., Parfenova, H., and Jaggar, J. H. (2011). Carbon monoxide as an endogenous vascular modulator. *Am. J. Physiol. Heart Circ. Physiol.* **301,** H1–H11.

Li, Z., Carter, J. D., Dailey, L. A., and Huang, Y. C. (2005). Pollutant particles produce vasoconstriction and enhance MAPK signaling via angiotensin type I receptor. *Environ. Health Perspect.* **113,** 1009–1014.

Lin, W., Huang, Y. W., Zhou, X. D., and Ma, Y. (2006). Toxicity of cerium oxide nanoparticles in human lung cancer cells. *Int. J. Toxicol.* **25,** 451–457.

Ma, J. Y., Young, S. H., Mercer, R. R., Barger, M., Schwegler-Berry, D., Ma, J. K., and Castranova, V. (2014). Interactive effects of cerium oxide and diesel exhaust nanoparticles on inducing pulmonary fibrosis. *Toxicol. Appl. Pharmacol.* **278,** 135–147.

Ma, J. Y., Zhao, H., Mercer, R. R., Barger, M., Rao, M., Meighan, T., Schwegler-Berry, D., Castranova, V., and Ma, J. K. (2011). Cerium oxide nanoparticle-induced pulmonary inflammation and alveolar macrophage functional change in rats. *Nanotoxicology* **5,** 312–325.

McDonald, J. D., Campen, M. J., Harrod, K. S., Seagrave, J., Seilkop, S. K., and Mauderly, J. L. (2011). Engine-operating load influences diesel exhaust composition and cardiopulmonary and immune responses. *Environ. Health Perspect.* **119,** 1136–1141.

Miller, A., Ahlstrand, G., Kittelson, D. B., and Zachariah, M. R. (2007). The fate of metal (Fe) during diesel combustion: Morphology, chemistry, and formation pathways of nanoparticles. *Combust. Flame* **149,** 129–143.

Mills, N. L., Tornqvist, H., Gonzalez, M. C., Vink, E., Robinson, S. D., Soderberg, S., Boon, N. A., Donaldson, K., Sandstrom, T., Blomberg, A., *et al.* (2007). Ischemic and thrombotic effects of dilute diesel-exhaust inhalation in men with coronary heart disease. *N. Engl. J. Med.* **357,** 1075–1082.

Nalabotu, S. K., Kolli, M. B., Triest, W. E., Ma, J. Y., Manne, N. D., Katta, A., Addagarla, H. S., Rice, K. M., and Blough, E. R. (2011). Intratracheal instillation of cerium oxide nanoparticles induces hepatic toxicity in male Sprague-Dawley rats. *Int. J. Nanomedicine* **6,** 2327–2335.

Nash, D. G., Swanson, N. B., Preston, W. T., Yelverton, T. L. B., Roberts, W. L., Wendt, J. O. L., and Linak, W. P. (2013). Environmental implications of iron fuel borne catalysts and their effects on diesel particulate formation and composition. *J. Aerosol. Sci.* **58,** 50–61.

Neeft, J. P. A., Makkee, M., and Moulijn, J. A. (1996). Diesel particulate emission control. *Fuel Process. Technol.* **47,** 1–69.

O'Brien, N., and Cummins, E. (2010). Nano-scale pollutants: Fate in Irish surface and drinking water regulatory systems. *Hum. Ecol. Risk Assess.* **16,** 847–872.

Park, B., Donaldson, K., Duffin, R., Tran, L., Kelly, F., Mudway, I., Morin, J. P., Guest, R., Jenkinson, P., Samaras, Z., *et al.* (2008a). Hazard and risk assessment of a nanoparticulate cerium oxide-based diesel fuel additive—A case study. *Inhal. Toxicol.* **20,** 547–566.

Park, B., Martin, P., Harris, C., Guest, R., Whittingham, A., Jenkinson, P., and Handley, J. (2007). Initial in vitro screening approach to investigate the potential health and environmental hazards of Envirox^{TM}—A nanoparticulate cerium oxide diesel fuel additive. *Part Fibre Toxicol.* **4,** 4–12.

Park, E. J., Choi, J., Park, Y. K., and Park, K. (2008b). Oxidative stress induced by cerium oxide nanoparticles in cultured BEAS-2B cells. *Toxicology* **245,** 90–100.

Peretz, A., Sullivan, J. H., Leotta, D. F., Trenga, C. A., Sands, F. N., Allen, J., Carlsten, C., Wilkinson, C. W., Gill, E. A., and Kaufman, J. D. (2008). Diesel exhaust inhalation elicits acute vasoconstriction in vivo. *Environ. Health Perspect.* **116,** 937–942.

Piao, Y., Liu, Y., and Xie, X. (2013). Change trends of organ weight background data in Sprague Dawley rats at different ages. *J. Toxicol. Pathol.* **26,** 29–34.

Ristovski, Z. D., Miljevic, B., Surawski, N. C., Morawska, L., Fong, K. M., Goh, F., and Yang, I. A. (2012). Respiratory health effects of diesel particulate matter. *Respirology* **17,** 201–212.

Sadauskas, E., Jacobsen, N. R., Danscher, G., Stoltenberg, M., Vogel, U., Larsen, A., Kreyling, W., and Wallin, H. (2009). Biodistribution of gold nanoparticles in mouse lung following intratracheal instillation. *Chem. Cent. J.* **3,** 16.

Salvi, S., Blomberg, A., Rudell, B., Kelly, F., Sandstrom, T., Holgate, S. T., and Frew, A. (1999). Acute inflammatory responses in the airways and peripheral blood after short-term exposure to diesel exhaust in healthy human volunteers. *Am. J. Respir. Crit. Care Med.* **159,** 702–709.

Shannahan, J. H., Kodavanti, U. P., and Brown, J. M. (2012). Manufactured and airborne nanoparticle cardiopulmonary interactions: A review of mechanisms and the possible contribution of mast cells. *Inhal. Toxicol.* **24,** 320–339.

Sharkhuu, T., Doerfler, D. L., Krantz, Q. T., Luebke, R. W., Linak, W. P., and Gilmour, M. I. (2010). Effects of prenatal diesel exhaust inhalation on pulmonary inflammation and development of specific immune responses. *Toxicol. Lett.* **196,** 12–20.

Skillas, G., Qian, Z., Baltensperger, U., Matter, U., and Burtscher, H. (2000). The influence of additives on the size distribution and composition of particles produced by diesel engines. *Combust. Sci. Technol.* **154,** 259–273.

Srinivas, A., Rao, P. J., Selvam, G., Murthy, P. B., and Reddy, P. N. (2011). Acute inhalation toxicity of cerium oxide nanoparticles in rats. *Toxicol. Lett.* **205,** 105–115.

Stanek, L. W., Brown, J. S., Stanek, J., Gift, J., and Costa, D. L. (2011). Air pollution toxicology—A brief review of the role of the science in shaping the current understanding of air pollution health risks. *Toxicol. Sci.* **120**(Suppl. 1), S8–S27.

Stayner, L., Dankovic, D., Smith, R., and Steenland, K. (1998). Predicted lung cancer risk among miners exposed to diesel exhaust particles. *Am. J. Ind. Med.* **34,** 207–219.

Wakefield, G., Wu, X., Gardener, M., Park, B., and Anderson, S. (2008). Envirox^{TM} fuel-borne catalyst: Developing and launching a nano-fuel additive. *Technol. Anal. Strat.* **20,** 127–136.

Wauters, A., Dreyfuss, C., Pochet, S., Hendrick, P., Berkenboom, G., van de Borne, P., and Argacha, J. F. (2013). Acute exposure to diesel exhaust impairs nitric oxide-mediated endothelial vasomotor function by increasing endothelial oxidative stress. *Hypertension* **62,** 352–358.

WHO. (2010). *World Health Organization Guidelines for Indoor Air Quality: Selected Pollutants*. Available at: http://www.euro.

who.int/__data/assets/pdf_file/0009/128169/e94535.pdf. Accessed October 8, 2014.

Wichers, L. B., Rowan, W. H., 3rd, Nolan, J. P., Ledbetter, A. D., McGee, J. K., Costa, D. L., and Watkinson, W. P. (2006). Particle deposition in spontaneously hypertensive rats exposed via whole-body inhalation: Measured and estimated dose. *Toxicol. Sci.* **93,** 400–410.

Yokel, R. A., Florence, R. L., Unrine, J. M., Tseng, M. T., Graham, U. M., Wu, P., Grulke, E. A., Sultana, R., Hardas, S. S., and Butterfield, D. A. (2009). Biodistribution and oxidative stress effects of a systemically-introduced commercial ceria engineered nanomaterial. *Nanotoxicology* **3,** 234–248.

Yoon, J., Kim, M., Song, S., and Chun, K. M. (2011). Calculation of mass-weighted distribution of diesel particulate matters using primary particle density. *J. Aerosol. Sci.* **42,** 419–427.

Zhang, J., Nazarenko, Y., Zhang, L., Calderon, L., Lee, K. B., Garfunkel, E., Schwander, S., Tetley, T. D., Chung, K. F., Porter, A. E., *et al.* (2013). Impacts of a nanosized ceria additive on diesel engine emissions of particulate and gaseous pollutants. *Environ. Sci. Technol.* **47,** 13077–13085.